LETTER

doi:10.1038/nature09554

A dimorphic pheromone circuit in *Drosophila* from sensory input to descending output

Vanessa Ruta[1], Sandeep Robert Datta[1]†, Maria Luisa Vasconcelos[1]†, Jessica Freeland[1], Loren L. Looger[2] & Richard Axel[1]

Drosophila **show innate olfactory-driven behaviours that are observed in naive animals without previous learning or experience, suggesting that the neural circuits that mediate these behaviours are genetically programmed. Despite the numerical simplicity of the fly nervous system, features of the anatomical organization of the fly brain often confound the delineation of these circuits. Here we identify a neural circuit responsive to cVA, a pheromone that elicits sexually dimorphic behaviours[1–4]. We have combined neural tracing using an improved photoactivatable green fluorescent protein (PA-GFP) with electrophysiology, optical imaging and laser-mediated microlesioning to map this circuit from the activation of sensory neurons in the antennae to the excitation of descending neurons in the ventral nerve cord. This circuit is concise and minimally comprises four neurons, connected by three synapses. Three of these neurons are overtly dimorphic and identify a male-specific neuropil that integrates inputs from multiple sensory systems and sends outputs to the ventral nerve cord. This neural pathway suggests a means by which a single pheromone can elicit different behaviours in the two sexes.**

The male pheromone 11-*cis*-vaccenyl acetate (cVA) elicits male–male aggression[4] and suppresses male courtship towards females as well as males[1–3]. In females, cVA activates the same sensory neurons to promote receptivity to males[2]. cVA-induced aggregation behaviour is shown by both sexes[5]. What neural circuits permit a single pheromone acting through the same set of sensory neurons to elicit several distinct and sexually dimorphic behavioural responses?

The sensory neurons that express the odorant receptor Or67d respond to cVA[2,6,7], and these neurons converge on the DA1 glomerulus in the antennal lobe[8,9]. Projection neurons (PNs) that innervate the DA1 glomerulus terminate in the lateral horn of the protocerebrum[10–12]. In previous experiments we showed that the DA1 axons are sexually dimorphic and reveal a male-specific ventral axonal arborization in the lateral horn[13]. This dimorphism by itself might explain the sexually dimorphic behaviours or, alternatively, it might presage iterative anatomical dimorphisms at each stage in the circuit to descending output. We therefore characterized a neural circuit that transmits information from the DA1 PNs to the ventral nerve cord. We restricted our analysis to neurons that express the sexually dimorphic transcription factor fruitless (Fru^M). Fru^M is expressed in both Or67d-expressing sensory neurons and DA1 PNs[14,15] and governs the development of dimorphic neural circuitry including the male-specific axonal arborization of DA1 PNs[13,16,17]. In addition Fru^M specifies many male-specific behaviours, including those that are mediated by cVA[14,15,18–22].

In initial experiments we used PA-GFP[23] to identify Fru+ third-order neurons whose dendritic processes are closely apposed to DA1 axon termini. We developed a strategy in which two-photon photoactivation is restricted to a small, circumscribed region of a neuron's axonal arborization with the expectation that this would label the postsynaptic cells by photoconversion of PA-GFP in their dendrites. To ensure that this limited activation could produce sufficient signal from the photoconverted fluorophore to illuminate third-order neurons and their most distal processes, we generated two new enhanced PA-GFPs, namely C3PA-GFP and SPA-GFP[24] (Supplementary Fig. 1).

Photoconversion of the DA1 glomerulus in flies expressing C3PA-GFP or SPA-GFP under the control of fru^{GAL4} (ref. 14) readily identified the axonal arborizations of the DA1 PNs (Fig. 1a). We then photoactivated the volume of neuropil circumscribing the DA1 axon termini and reproducibly labelled four clusters of presumptive third-order neurons in the lateral horn of male flies ($n = 7$; Fig. 1b and Supplementary Fig. 2). Labelling of the two dorsal clusters, DC1 and DC2, was observed only in males; the clusters were either absent in the female or lacked projections into the ventral lateral horn ($n = 6$; Fig. 1c). The lateral cluster LC1 was present in the two sexes but was dimorphic in both number and projection pattern (males 25.8 ± 3.4 (mean $\pm$ s.d.), $n = 6$; females 15.8 ± 3.0, $n = 5$). LC2 did not show an apparent numeric or anatomical dimorphism (males 13.0 ± 2.8, $n = 8$; females 13.3 ± 2.1, $n = 8$). Photoactivation of DA1 axon terminals in male flies that express C3PA-GFP pan-neuronally labelled few additional neurons and suggests that these four Fru+ clusters constitute the major potential recipients of DA1 input (Supplementary Fig. 3).

These photoactivation experiments identify clusters of third-order neurons in the lateral horn that are anatomically poised to propagate dimorphic responses to cVA. However, anatomical proximity does not ensure functional connectivity. We therefore developed a method to specifically activate individual glomeruli and simultaneously record from presumptive downstream neurons to determine whether the lateral horn clusters that we identify receive excitatory input from DA1 PNs. We selectively stimulated DA1 PNs by positioning a fine glass electrode in the centre of the DA1 glomerulus and iontophoresing acetylcholine, the neurotransmitter that excites PNs[25], into the glomerular neuropil (Fig. 2a). Varying the iontophoretic voltage allowed us to vary the frequency of elicited action potentials systematically in DA1 PNs up to 250 Hz (Fig. 2b), a value close to the upper limit of cVA-elicited responses measured in these PNs[13,26]. Activation of the DA1 glomerulus over this voltage range excited DA1 PNs specifically and elicited no response in PNs innervating other glomeruli in the antennal lobe (Fig. 2b). Stimulation of the neighbouring glomeruli, VA1d and VA1lm, similarly elicited the specific excitation of their cognate PNs but did not activate DA1 PNs (Fig. 2b).

We then examined whether stimulation of the DA1 glomerulus would result in the excitation of neurons within the four clusters in the lateral horn that we identified, a result indicative of functional synaptic connections with DA1 PNs. We expressed the genetically encoded calcium indicator GCaMP3 (ref. 27) in Fru+ neurons in male flies and used two-photon imaging to monitor increases in Ca^{2+} concentration in the lateral horn clusters in response to DA1 excitation. Stimulation of the DA1 glomerulus elicited large increases in Ca^{2+} in neurons within the DC1 and LC1 clusters, with a far weaker response being observed in LC2 (Fig. 2c). The small DC2 cluster is difficult to identify reliably because of the low basal fluorescence of GCaMP3; it

[1]Department of Biochemistry and Molecular Biophysics and the Howard Hughes Medical Institute, College of Physicians and Surgeons, Columbia University, New York, New York 10032, USA. [2]Howard Hughes Medical Institute, Janelia Farm Research Campus, Ashburn, Virginia 20147, USA. †Present addresses: Department of Neurobiology, Harvard Medical School, Boston, Massachusetts 02115, USA (S.R.D.); Champalimaud Neuroscience Programme, Instituto Gulbenkian de Ciência, Rua da Quinta Grande, 6, P-2780-156 Oeiras, Portugal (M.L.V.).

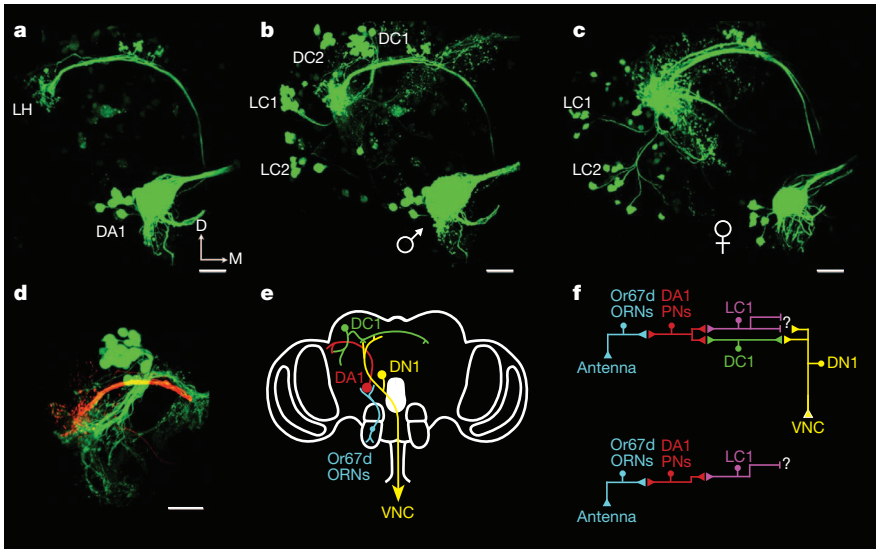

Figure 1 | Photoactivation identifies dimorphic lateral horn neurons. **a**, Photoactivation of the DA1 glomerulus in a male fly labels DA1 PNs including their axonal arborization in the lateral horn (LH). **b**, Photoactivation of a volume circumscribing the DA1 axon terminals labels dorsal (DC1 and DC2) and lateral (LC1 and LC2) LH neuronal clusters in the male. **c**, Photoactivation of the DA1 axon terminals analogous to **b** in the female labels only lateral LH clusters. Note that LC1 neurons are more numerous in males and that DC1 and DC2 are absent in females. **d**, DA1 axons and DC1 dendrites interdigitate within the LH. DA1 axons were labelled by electroporation of the DA1 glomerulus with Texas Red dextran, and DC1 neurons were labelled by direct photoactivation of the fasciculated DC1 dendritic processes. For clarity, the basal fluorescence from non-photoactivated neurons has been masked in **d**. All images are *z*-projections acquired by two-photon laser scanning microscopy of photoactivated neurons in which fru^{GAL4} directs C3PA-GFP or SPA-GFP expression. Scale bars, 20 μm. Dorsal (D) and medial (M) axes are indicated. All images are oriented similarly to that in **a**. **e**, Diagram of the male fly brain illustrating neurons that constitute the cVA-responsive circuit defined in this study. **f**, Circuit diagrams for identified dimorphic cVA pathways in the male (top) and female (bottom).

was therefore not examined by optical imaging. The Ca^{2+} response in DC1 was specific for DA1 activation and was not observed when the stimulating electrode was repositioned in two neighbouring glomeruli, VA1d and VA1lm ($n = 5$, data not shown). These optical imaging experiments demonstrate that neurons within the DC1 and LC1 clusters extend processes in anatomical proximity to the DA1 axons and receive excitatory input from DA1 PNs (Fig. 1e, f). Immunostaining indicated that neurons within the LC1 cluster produce the inhibitory neurotransmitter GABA (γ-aminobutyric acid; Supplementary Fig. 4). Electrophysiological experiments suggested that DC1 neurons are excitatory (see below) but the neurotransmitter remains unknown.

We focused on the male-specific DC1 neurons to define a cVA-responsive circuit. The DC1 cluster consists of 19.7 ± 2.3 (mean ± s.d.) cell bodies ($n = 10$) in a spatially stereotyped location in the dorsal aspect of the anterior protocerebrum. Double labelling experiments revealed that the DC1 processes interdigitate richly with DA1 axons (Fig. 1d) in the lateral horn. Photoactivation of single DC1 cell bodies indicated that the cluster is composed of several anatomical classes of neurons characterized by distinct branch patterns within the protocerebrum (Supplementary Fig. 5) that are likely to receive and integrate inputs from both olfactory and non-olfactory brain centres (Supplementary Fig. 6).

We performed electrophysiological recordings to examine the response of DC1 neurons to both DA1 stimulation and cVA exposure. Selective stimulation of the DA1 glomerulus evoked action potentials in 66% of male-specific DC1 neurons ($n = 73$ neurons) recorded in the loose patch configuration (Fig. 2d, g). Among responsive DC1 neurons, we observed that the sensitivity to DA1 stimulation differed. This functional heterogeneity within the DC1 cluster observed by both electrical and optical recording was consistent with the anatomical heterogeneity of dendritic fields in the lateral horn observed for single DC1 neurons (Supplementary Fig. 5).

In accord with the imaging experiments, the electrophysiological response of DC1 neurons is selectively tuned to DA1 input. After recording the response of a DC1 neuron to DA1 stimulation, we repositioned the stimulating electrode into 6–11 other superficial glomeruli located throughout the antennal lobe ($n = 8$).We observed that DC1 neurons activated by minimal DA1 stimulation (0.3 V) were either weakly excited or unresponsive to strong stimulation (4 V) of other glomeruli (Fig. 2e). Stimulation of the Fru+ VA1lm glomerulus ($n = 15$) failed to excite DC1 neurons despite the close proximity of DA1 and VA1lm axons[12]. These observations demonstrate the specificity of glomerular excitation and reveal that olfactory input to DC1 is mediated largely by the DA1 glomerulus and not by the activation of at least 11 other glomeruli, suggesting that DC1 neurons receive olfactory stimulation only from cVA. We next recorded cVA-evoked responses from DC1 neurons in an intact fly preparation. We observed that 62% of DC1 neurons were responsive to cVA over a range of concentrations (Fig. 2f, g; $n = 71$). The input–output relationship of DC1 neurons was similar whether action potentials were evoked in DA1 PNs through direct glomerular stimulation or by pheromonal excitation of the antenna, suggesting that DC1 neurons are excited primarily by means of DA1 input (Fig. 2g). Both Or67d-expressing sensory neurons and DA1 PNs have been shown to be selectively tuned to cVA[6,7,26]. DC1 neurons showed similar odorant selectivity (Fig. 2f) and fired only weakly in response to stimulation of the antenna with a cocktail of ten fruit-derived odorants that excite a majority of glomeruli (Supplementary Fig. 7). Thus, DC1 neurons are likely to receive direct excitatory feedforward input from DA1 PNs and respond selectively to cVA.

Photoactivation of PA-GFP in presynaptic DA1 axonal arborizations, in concert with electrophysiology, has identified postsynaptic third-order neurons in the lateral horn that are responsive to cVA. The iterative use of this strategy could allow us to define the complete cVA circuit from sensory input to descending output. Tracing of photoactivated DC1 axons ($n = 15$) revealed that they terminate proximally within a triangular neuropil in the lateral protocerebrum (the lateral triangle) and extend distal processes to a previously uncharacterized tract within the superior medial protocerebrum (the SMP tract; Fig. 3a). The lateral triangle and SMP tract are sexually dimorphic neuropils that are absent in females (Fig. 3c).

Photoactivation of the terminal arborizations of DC1 axons was performed to identify neurons innervating the lateral triangle and

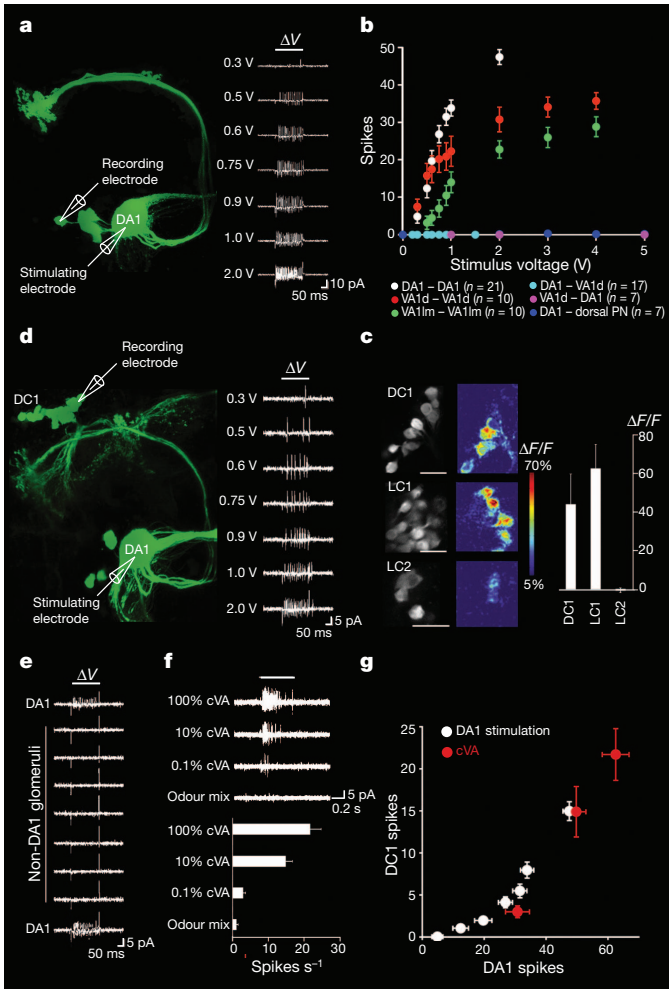

Figure 2 | DC1 neurons synapse with DA1 PNs and are selectively tuned to cVA. **a**, Selective stimulation of single glomeruli through iontophoresis of acetylcholine shown schematically (left). Right: stimulation of the DA1 glomerulus at the indicated voltages evokes graded responses in DA1 PNs recorded in the loose patch configuration. **b**, Spike count recorded in PNs in response to stimulation of a single glomerulus at the indicated voltages. **c**, Optical recordings of Ca^{2+}-mediated changes in fluorescence ($\Delta F/F$) in LH clusters expressing GCaMP3 under the control of fru^{GAL4}, evoked by stimulation of the DA1 glomerulus (left). Scale bars, 10 μm. Right: bar graph showing mean and s.e.m. ($n = 5$) normalized fluorescence changes in LH clusters evoked by simulation of DA1. **d**, Diagram of the recording configuration (left) used to measure the response of a DC1 neuron to stimulation of the DA1 glomerulus at indicated voltages (right). **e**, The response of a DC1 neuron to sequential stimulation of the DA1 glomerulus, seven superficial glomeruli, and then the DA1 glomerulus. Note a residual stimulus artefact at the beginning and end of the 200-ms stimulation. **f**, Spikes evoked in DC1 neurons by exposure of antenna for 1 s to 0.1% cVA ($n = 25$), 10% cVA ($n = 47$), 100% cVA ($n = 27$) or a mix of ten general odorants ($n = 23$). **g**, Input–output relationship of DA1–DC1 neurons observed on stimulation of the DA1 glomerulus for 200 ms at the voltages indicated in **d** ($n = 56$, white) or after an exposure of the antenna for 1 s to different concentrations of cVA (red). All plotted values are means ± s.e.m. for responsive DC1 neurons.

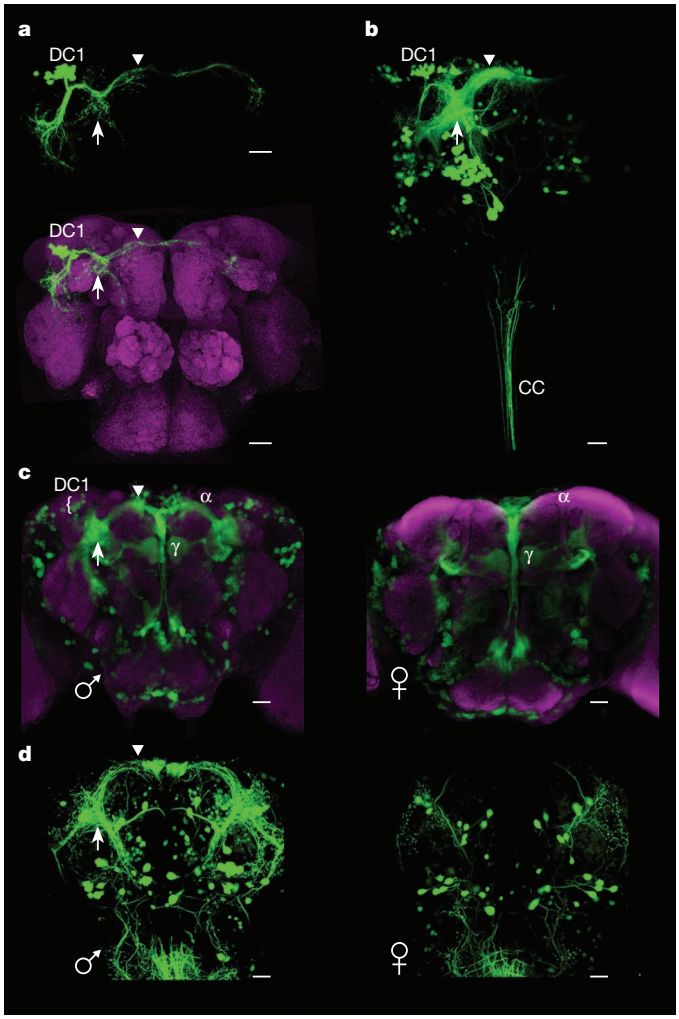

Figure 3 | DC1 and descending neurons innervate Fru+ dimorphic neuropil. **a**, Direct photoactivation of the DC1 cluster (green, top) followed by counterstaining of neuropil with the nc82 antibody (magenta, bottom) reveals terminations in the lateral triangle (arrow) and SMP tract (arrowhead) and define a Fru+ integrative neuropil. For clarity, background fluorescence from non-photoactivated neurons has been masked in **a**. **b**, Photoactivation of the DC1 axon terminals in the lateral triangle (arrow) labels a large population of Fru+ neurons including fibres that project to the SMP tract (arrowhead) and fibres that descend into the cervical connectives (CC). **c**, Images of a male brain (left) and a female brain (right) in which Fru+ neurons express CD8-GFP (green). The neuropil is counterstained with the nc82 antibody (magenta). These images highlight dimorphic neural structures including the DC1 cluster, the lateral triangle (arrow) and SMP tract (arrowhead). Equivalent 20-μm confocal *z*-sections were defined by using the α-lobes and γ-lobes of the mushroom bodies as landmarks. **d**, Photoactivation of the cervical connectives in a male fly (left) and a female fly (right) labels descending neuron cell bodies and reveals dimorphic projections that innervate the lateral triangle (arrow) and SMP tract (arrowhead). Scale bars, 20 μm.

SMP tract ($n = 6$; Fig. 3b). We observed dense labelling in these structures arising from the rich male-specific projections of multiple classes of Fru+ neurons. Dimorphic LC1 neurons that receive direct innervation from DA1 PNs send inhibitory projections to the lateral triangle and SMP tract (Fig. 1e, f and Supplementary Fig. 2). We also observed dimorphic mAL neurons extending from the suboesophageal ganglion (SOG) and terminating within these neuropils[16]. In addition, these neuropils are innervated by male-specific P1 interneurons implicated in the initiation of male courtship behaviour[17]. Thus, the lateral triangle and SMP tract receive dimorphic projections from several brain regions including other sensory processing areas, suggesting that these neuropils may integrate sex-specific information from multiple sensory systems.

Several neurons that innervate the lateral triangle and SMP tract also extend processes that descend into the ventral nerve cord, suggesting that these potential fourth-order descending neurons may transmit information from cVA-responsive sensory neurons to the ganglia of the ventral nerve cord. Descending neurons that innervate the lateral triangle and SMP tract were characterized by photoactivation of the cervical connectives conveying neural signals from the brain to the ventral nerve cord (Fig. 3d). In the brain, the processes of these descending neurons showed a marked dimorphism that was apparent in their

extensive innervation of the male-specific SMP tract and lateral triangle (Fig. 3d). A descending neuron, DN1, absent in females, was observed in the ventral posterior aspect of the male brain, at the midline. Labelling of this male-specific cell body revealed short processes terminating within the lateral triangle and SMP tract, and a long descending process entering the ventral nerve cord and terminating within the thoracic and abdominal ganglia (Fig. 4a, b). Electroporation of DN1 with Texas Red dextran, followed by photoactivation of the DC1 cluster, revealed extensive intermingling of the green DC1 axons with the red dendrites of the descending neuron (Fig. 4a). This suggests that this descending neuron is anatomically poised to make direct synaptic contacts with third-order, cVA-responsive DC1 neurons.

We performed whole-cell patch clamp recordings on DN1 to discern whether it transmits pheromonal information to the ventral nerve cord. We observed that in response to either exposure of the antenna to cVA or direct stimulation of the DA1 glomerulus, DN1 received a barrage of excitatory postsynaptic potentials (EPSPs) bringing its membrane potential close to or past threshold ($n = 6$; Fig. 4c, f). To determine whether this response was mediated by DC1 neurons, we devised a microlesion technique exploiting the spatial precision of a two-photon laser to effectively sever DC1 inputs into the lateral triangle and SMP tract (Fig. 4d). Optical recordings revealed that microlesioning of DC1 dendrites resulted in the immediate and selective loss of DC1 responses to DA1 stimulation without affecting the excitation of neighbouring LC1 dendrites and cell bodies ($n = 5$; Fig. 4e). Severing the connections between DA1 and DC1 resulted in an almost complete loss of the response of DN1 to stimulation of DA1 ($n = 6$; Fig. 4f, g). The response of this descending neuron was far weaker than the response of early neural participants in this circuit. However, the observation that two-photon-mediated microlesions in DC1 resulted in a decrease of more than 70% in the DN1 response to stimulation of DA1 suggests that, despite its weak excitation, DN1 is a component of this circuit. A more potent response may require a more natural setting that integrates pheromonal input with other sensory signals. Taken together, these experiments suggest that male-specific DC1 neurons excite the male-specific DN1 through synaptic connections within the dimorphic lateral triangle and SMP tract. Thus, olfactory information may be processed by as few as three synapses within the brain before descending to initiate motor programs within the ganglia of the ventral nerve cord (Fig. 1e, f). Although we cannot yet define a behaviour elicited by this circuit, we presume that it mediates a component of the innate behavioural repertoire initiated by cVA.

This cVA-responsive circuit provides insights into the mechanism by which sensory information received by the antenna may be translated into motor output. First, the circuit is concise: as few as four neuronal clusters and three synapses bring pheromonal signals from the periphery to the ganglia of the nerve cord. This minimal circuit assumes monosynaptic connections between the neurons that we have identified. This circuit is shallow but seems to include adequate synaptic connections to permit the integration of olfactory and non-olfactory information. Third-order lateral horn neurons reveal a capacity for

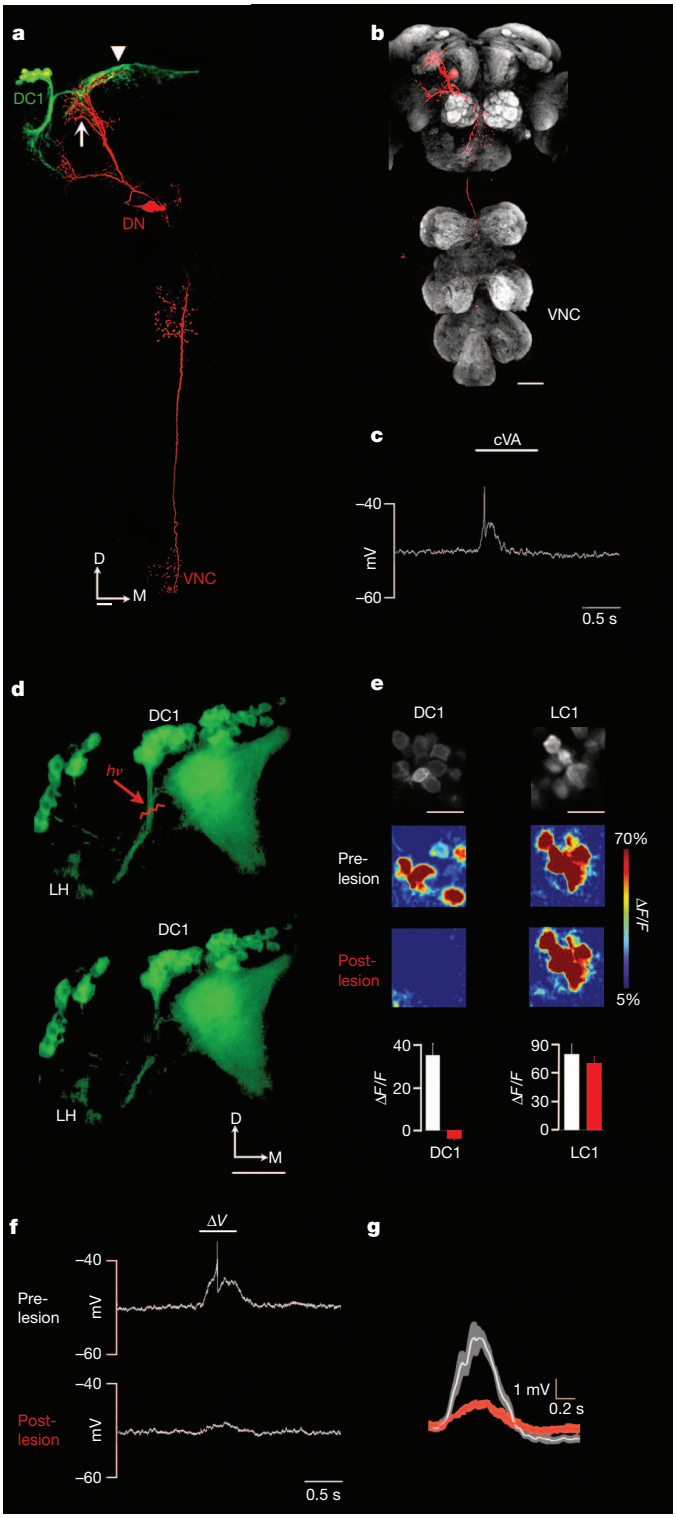

Figure 4 | DC1 neurons excite DN1, a cVA-responsive, male-specific descending neuron. **a**, DC1 axons (labelled green by direct photoactivation) interdigitate with the dendrites of DN1 (labelled by single-cell electroporation of Texas Red dextran) in the lateral triangle (arrow) and SMP tract (arrowhead). Scale bar, 20 µm. Dorsal (D) and medial (M) axes are indicated. **b**, The axon of a dye-filled DN1 (red) terminates within the ventral nerve cord (VNC) in a male fly whose neuropil has been counterstained with the nc82 antibody (grey). Scale bar, 80 µm. **c**, Intracellular recording of DN1 in response to an application of 10% cVA to the antenna for 1 s. **d**, Two-photon laser-mediated microlesioning severs DC1 dendritic processes as they exit from the lateral horn (LH). Images of Fru+ neurons expressing CD8-GFP before (top) and after (bottom) microlesioning. The laser was targeted to DC1 neuronal processes at the position indicated by the red arrow (*hv*). Scale bar, 20 µm. **e**, Microlesioning of DC1 processes results in the loss of Ca^{2+} responses evoked by DA1 stimulation in DC1 but not LC1 cell bodies. Fluorescence changes ($\Delta F/F$) in response to stimulation of the DA1 glomerulus were recorded in DC1 and LC1 neurons expressing GCaMP3 under the control of fru^{GAL4}. The bar graphs (bottom) show normalized changes in fluorescence (means and s.e.m.; $n = 5$ flies) for all DC1 or LC1 cell bodies in the same *z* plane before (white) and after (red) microlesioning of DC1 processes. **f**, Intracellular recording of DN1 in response to stimulation of the DA1 glomerulus for 500 ms before (top) and after (bottom) microlesioning of DC1 processes. **g**, Average change in synaptic potential recorded in DN1 in response to stimulation of DA1, before (white) and after (red) microlesioning of DC1 processes ($n = 6$, mean ± s.e.m.). DN1 responses have been digitally low-pass filtered (Butterworth, 10 Hz) to remove action potentials.

multisensory integration with inputs to the DC1 cluster from the SOG and from the optic lobe. The lateral triangle and SMP tract also integrate sensory inputs from DC1 and LC1 as well as inhibitory projections from the SOG[16]. This integration provides the opportunity for other sensory signals emanating from a cVA-scented fly to modulate the response to the pheromone.

Second, multiple neural components within the circuit are anatomically dimorphic, and this could explain the different behaviours elicited by cVA in males and females. The initial neural components of the circuit, Or67d-expressing sensory neurons and DA1 PNs, are dedicated to the receipt of a singular olfactory stimulus, cVA, and are equally responsive to the pheromone in the two sexes[2,13]. However, dimorphisms are observed in the synaptic connections between the PNs and the third-order lateral horn neurons and define a node from which sex-specific neural pathways emanate. The DA1 PNs reveal dimorphic axon arborizations[13], but this dimorphism is only one component of a highly dimorphic circuit. These dimorphic arborizations synapse with male-specific DC1 neurons that send axons to a male-specific neuropil (the lateral triangle and SMP tract). One output of this neuropil is a male-specific descending neuron, DN1 (Fig. 1e, f). This circuit is likely to participate in the generation of cVA-elicited behaviours observed only in males. The identification of a sex-specific circuit including extensive neuropils present only in males suggests pathways for dimorphic behaviours that differ from earlier proposals that invoke the differential activation of circuits that are common to the two sexes[28,29]. DA1 PNs also synapse onto the cluster of LC1 neurons that are present in both sexes but are numerically and anatomically dimorphic. The multiple dimorphic targets of a singular olfactory input could explain how a pheromone acting through the same sensory inputs may elicit different behaviours in the two sexes.

METHODS SUMMARY

Optical tracing of neurons was performed on flies that express fru^{GAL4} (ref. 20) driving the expression of C3PA-GFP or SPA-GFP. Photoactivation was performed essentially as described[13] except that regions of interest for photoconversion were defined manually in three dimensions by using masks generated in Prairie View software (Prairie Technologies). We identified lateral horn neurons receiving functional input from DA1 PNs by first photoactivating the DA1 glomerulus to reveal DA1 axons. We then defined a photoactivation mask circumscribing all DA1 axon terminals in the lateral horn and exposed this masked volume to photoconverting 710-nm light. Direct photoactivation of the DC1 cluster was achieved through irradiation of a small volume (typically about 2–5 μm on each axis) centred on the fasciculated dendritic processes as they exit from the lateral horn. We selectively excited individual glomeruli by positioning glass electrodes (7–8 MΩ) filled with 2 mM acetylcholine in the centre of superficial glomeruli. Voltage pulses (200 or 500 ms) were then applied by means of a Grass stimulator to excite the impaled glomerulus. For microlesioning experiments, we targeted a small area (about 1 μm × 2 μm) centred on the tightly fasciculated DC1 processes proximal to where they bifurcate and innervate the lateral triangle by using a high zoom (×8). We then applied one to four pulses of 800-nm laser light (75–90 mW at the back aperture) until we observed a physical discontinuity.

Full Methods and any associated references are available in the online version of the paper at www.nature.com/nature.

Received 8 July; accepted 29 September 2010.

1. Ejima, A. *et al.* Generalization of courtship learning in *Drosophila* is mediated by *cis*-vaccenyl acetate. *Curr. Biol.* **17,** 599–605 (2007).
2. Kurtovic, A., Widmer, A. & Dickson, B. J. A single class of olfactory neurons mediates behavioural responses to a *Drosophila* sex pheromone. *Nature* **446,** 542–546 (2007).
3. Billeter, J. C., Atallah, J., Krupp, J. J., Millar, J. G. & Levine, J. D. Specialized cells tag sexual and species identity in *Drosophila melanogaster. Nature* **461,** 987–991 (2009).
4. Wang, L. & Anderson, D. J. Identification of an aggression-promoting pheromone and its receptor neurons in *Drosophila. Nature* **463,** 227–231 (2010).
5. Bartelt, R. J., Schaner, A. M. & Jackson, L. L. *Cis*-vaccenyl acetate as an aggregation pheromone in *Drosophila melanogaster. J. Chem. Ecol.* **11,** 1747–1756 (1985).
6. Clyne, P., Grant, A., O'Connell, R. & Carlson, J. R. Odorant response of individual sensilla on the *Drosophila* antenna. *Invert. Neurosci.* **3,** 127–135 (1997).
7. van der Goes van Naters, W. & Carlson, J. R. Receptors and neurons for fly odors in *Drosophila. Curr. Biol.* **17,** 606–612 (2007).
8. Couto, A., Alenius, M. & Dickson, B. J. Molecular, anatomical, and functional organization of the *Drosophila* olfactory system. *Curr. Biol.* **15,** 1535–1547 (2005).
9. Fishilevich, E. & Vosshall, L. B. Genetic and functional subdivision of the *Drosophila* antennal lobe. *Curr. Biol.* **15,** 1548–1553 (2005).
10. Marin, E. C., Jefferis, G. S., Komiyama, T., Zhu, H. & Luo, L. Representation of the glomerular olfactory map in the *Drosophila* brain. *Cell* **109,** 243–255 (2002).
11. Wong, A. M., Wang, J. W. & Axel, R. Spatial representation of the glomerular map in the *Drosophila* protocerebrum. *Cell* **109,** 229–241 (2002).
12. Jefferis, G. S. *et al.* Comprehensive maps of *Drosophila* higher olfactory centers: spatially segregated fruit and pheromone representation. *Cell* **128,** 1187–1203 (2007).
13. Datta, S. R. *et al.* The *Drosophila* pheromone cVA activates a sexually dimorphic neural circuit. *Nature* **452,** 473–477 (2008).
14. Stockinger, P., Kvitsiani, D., Rotkopf, S., Tirian, L. & Dickson, B. J. Neural circuitry that governs *Drosophila* male courtship behavior. *Cell* **121,** 795–807 (2005).
15. Manoli, D. S. *et al.* Male-specific *fruitless* specifies the neural substrates of *Drosophila* courtship behaviour. *Nature* **436,** 395–400 (2005).
16. Kimura, K., Ote, M., Tazawa, T. & Yamamoto, D. Fruitless specifies sexually dimorphic neural circuitry in the *Drosophila* brain. *Nature* **438,** 229–233 (2005).
17. Kimura, K., Hachiya, T., Koganezawa, M., Tazawa, T. & Yamamoto, D. Fruitless and doublesex coordinate to generate male-specific neurons that can initiate courtship. *Neuron* **59,** 759–769 (2008).
18. Ryner, L. C. *et al.* Control of male sexual behavior and sexual orientation in *Drosophila* by the *fruitless* gene. *Cell* **87,** 1079–1089 (1996).
19. Demir, E. & Dickson, B. J. *fruitless* splicing specifies male courtship behavior in *Drosophila. Cell* **121,** 785–794 (2005).
20. Vrontou, E., Nilsen, S. P., Demir, E., Kravitz, E. A. & Dickson, B. J. *fruitless* regulates aggression and dominance in *Drosophila. Nature Neurosci.* **9,** 1469–1471 (2006).
21. Billeter, J. C. *et al.* Isoform-specific control of male neuronal differentiation and behavior in *Drosophila* by the *fruitless* gene. *Curr. Biol.* **16,** 1063–1076 (2006).
22. Chan, Y. B. & Kravitz, E. A. Specific subgroups of FruM neurons control sexually dimorphic patterns of aggression in *Drosophila melanogaster. Proc. Natl Acad. Sci. USA* **104,** 19577–19582 (2007).
23. Patterson, G. H. & Lippincott-Schwartz, J. A photoactivatable GFP for selective photolabeling of proteins and cells. *Science* **297,** 1873–1877 (2002).
24. Shaner, N. C., Patterson, G. H. & Davidson, M. W. Advances in fluorescent protein technology. *J. Cell Sci.* **120,** 4247–4260 (2007).
25. Kazama, H. & Wilson, R. I. Homeostatic matching and nonlinear amplification at identified central synapses. *Neuron* **58,** 401–413 (2008).
26. Schlief, M. L. & Wilson, R. I. Olfactory processing and behavior downstream from highly selective receptor neurons. *Nature Neurosci.* **10,** 623–630 (2007).
27. Tian, L. *et al.* Imaging neural activity in worms, flies and mice with improved GCaMP calcium indicators. *Nature Methods* **6,** 875–881 (2009).
28. Dulac, C. & Kimchi, T. Neural mechanisms underlying sex-specific behaviors in vertebrates. *Curr. Opin. Neurobiol.* **17,** 675–683 (2007).
29. Clyne, J. D. & Miesenbock, G. Sex-specific control and tuning of the pattern generator for courtship song in *Drosophila. Cell* **133,** 354–363 (2008).

Supplementary Information is linked to the online version of the paper at www.nature.com/nature.

Acknowledgements We thank T. Jessell, C. Zuker and members of the Axel laboratory for discussion and comments on this manuscript; J. Flores for technical assistance; B. Dickson for reagents; P. Kisloff for assistance in the preparation of this manuscript; and M. Gutierrez and A. Nemes for general laboratory support. This work was funded in part by a grant from the Foundation for the National Institutes of Health through the Grand Challenges in Global Health Initiative. Further financial support was provided by the Helen Hay Whitney Foundation (V.R. and S.R.D.), the Burroughs Welcome Fund (S.R.D.) and the Howard Hughes Medical Institute (R.A. and L.L.L.).

Author Contributions V.R., S.R.D., M.L.V. and R.A. conceived of the project and contributed to its progression. V.R. performed all the experiments, with the early participation of M.L.V. S.R.D. developed new photoactivatable fluorophores. L.L.L. developed GCaMP3. J.F. performed immunochemistry. R.A. provided guidance and wrote the paper with V.R., S.R.D., M.L.V. and L.L.L.

Author Information Reprints and permissions information is available at www.nature.com/reprints. The authors declare no competing financial interests. Readers are welcome to comment on the online version of this article at www.nature.com/nature. Correspondence and requests for materials should be addressed to R.A. (ra27@columbia.edu).

METHODS

Generation of C3PA-GFP and SPA-GFP. The optimized photoconvertible fluorophores C3PA-GFP and SPA-GFP were identified as part of a screen of mutations in the canonical photoconvertible fluorophore PA-GFP[23] with improved diffusional and folding properties. The screen (details of which are available from S.R.D.) included the analysis of previously described mutants of GFP for enhanced photoconversion in our system. C3PA-GFP incorporates three additional mutations (F99S, M153T and V163A) initially identified in the 'Cycle 3' mutant of GFP[30]. V163A was originally incorporated into the first-generation PA-GFP molecule[23]. SPA-GFP incorporates nine mutations (S30R, Y39N, A206V, M153T, Y145F, V163A, I171V, F99S and N105T) identified in the 'Superfolder' mutant of eGFP[24,31]. The mutations in C3PA-GFP and SPA-GFP do not include the 'eGFP' mutations F64L and S65T, which disrupt the ability of PA-GFP to undergo photoconversion.

Fly stocks. The GH146-Gal4 and MZ19-Gal4 driver lines used to label PNs have been described previously[10–12,32,33]. fru^{GAL4} (ref. 14) was a gift from B. Dickson. UAS-C3PA-GFP and UAS-SPA-GFP were generated by subcloning into pUAST. UAS-GCaMP3 (ref. 27) was generated by the insertion of *GCaMP3* cDNA into pUAST attB.

Imaging. We performed all imaging experiments on an Ultima two-photon laser scanning microscope (Prairie Technologies) equipped with galvanometers driving either a Coherent Chameleon XR or Chameleon Ultra II Ti:sapphire laser. Fluorescence was detected with either photomultiplier-tube or GaAsP photodiode (Hamamatsu) detectors. Images were acquired with either an Olympus 60× 0.9 numerical aperture or 1.1 numerical aperture objective at 512 pixels × 512 pixels resolution and 1-μm steps.

Labelling neurons through photoactivation. For photoactivation experiments we generated flies bearing fru^{GAL4} and two or three copies of UAS-C3PA-GFP or UAS-SPA-GFP. In some optical tracing experiments we used flies that contained one copy of UAS-C3PA-GFP and two copies of UAS-SPA-GFP. Although the basal fluorescence of C3PA-GFP is higher than that of SPA-GFP (Supplementary Fig. 1), the overall contrast of photoactivated neurons was essentially equivalent when the two fluorophores were used. C3PA-GFP and SPA-GFP were therefore often used interchangeably.

Photoactivation was performed on adult flies aged 12–24 h after eclosion. We initially imaged dissected brains at 925 nm (a wavelength at which photoconversion is relatively inefficient) to define two-dimensional or three-dimensional photoactivation masks of the appropriate neural targets using Prairie View software. We generated three-dimensional masks by defining a two-dimensional mask for each section of a *z*-series taken every 1–2 μm. Photoactivation of this masked volume was then achieved through two or three cycles of exposure to 710-nm laser light, a wavelength that more efficiently converts the fluorophore. We interposed a 'rest' period between each photoactivation cycle to allow diffusion of the photoconverted fluorophore into more distal neural processes and minimize photodamage. As a result of unavoidable variations in the orientation and optical accessibility of each brain, photoactivation powers and exposure times were determined empirically before each experiment for a single *z*-section of the masked target neuropil. Powers were typically between 5 and 30 mW (measured at the back aperture of the objective), depending most critically on the depth of the neural target. Exposure times were determined by adjusting the number of averaged images acquired for a given masked region.

We identified lateral horn neurons that receive functional input from DA1 PNs by first photoactivating the DA1 glomerulus as described previously[13] to reveal the DA1 PN axonal arborization. We then manually defined a three-dimensional mask circumscribing the photoactivated DA1 axon terminals in the lateral horn in Prairie View (Prairie Technologies). The mask included an additional approximately 1 μm around the perimeter of photoactivated axon terminals to ensure more intense exposure of postsynaptic processes to photoconverting light. Photoconversion was achieved by exposing the masked volume in the lateral horn to two or three photoactivation cycles (30-s intervals, 30–60 rounds per cycle).

Direct photoactivation of individual lateral horn clusters, including DC1, was achieved through the irradiation of a small volume (typically about 2–5 μm on each axis) centred on the fasiculated processes that lead to the cell bodies. This masked volume was then subject to two or three photoactivation cycles (5–10-s intervals, 90–120 rounds per cycle). We used the same photoactivation protocol for labelling single neurons except that the photoactivation mask was defined for a single *z*-plane centred on the cell body.

We identified neurons with processes that interdigitate with DC1 axons by first directly photoactivating the DC1 cluster as described above. This initial photoactivation labelled DC1 axons innervating the lateral triangle and SMP tract. We then defined a photoactivation mask around the DC1 axon terminals in the lateral triangle to label neurons whose processes lie in close anatomical proximity. DC1 boutons are small and spatially distributed within the lateral triangle and SMP tract. We defined this photactivation mask as the minimum volume encompassing all the DC1 boutons within the lateral triangle. Consequently, we photoactivated a somewhat larger volume of neuropil than if we had defined separate masks for each individual DC1 bouton. Photoconversion was achieved by exposing the masked volume in the lateral triangle to two or three photoactivation cycles (30-s intervals, 30–60 rounds per cycle). Other photoactivation experiments reveal that most neurons that innervate the SMP tract seem to have terminals in the lateral triangle (data not shown). In accord with this observation, we label a qualitatively similar set of neurons when we restrict our photoactivation to DC1 axon terminals in the SMP tract rather than the lateral triangle.

We labelled all Fru+ descending neurons in a preparation in which we dissected the entire central nervous system of the fly, paying particular attention to preserving the cervical connectives that link the brain to the ventral nerve cord. We then defined a photoactivation mask encompassing the full width and depth of the cervical connectives and about 30–50 μm in length. The masked cervical connectives were then subject to two or three photoactivation cycles (30-s intervals, 60–90 rounds per cycle).

Image processing. Maximum-intensity *z*-projections of *z*-stacks were generated in ImageJ (NIH) or Imaris (Bitplane). We masked images of photoactivated single neurons and individual neural clusters in Imaris or Adobe Photoshop to permit a clearer visualization of projection patterns. This procedure removed weak background fluorescence arising primarily from cell bodies and (less frequently) the processes of non-photoactivated neurons that would otherwise obscure photoactivated projection patterns in maximum-intensity *z*-projections. We emphasize that we did not mask images of photoactivated neuropils (lateral horn and lateral triangle and SMP tract; Figs 1a–c and 3b) and descending neurons (Fig. 3d) in which we examined collections of neurons labelled by virtue of their projections into the photoactivation target. In addition, we did not mask images in which we compared the fluorescent signal of different photoactivatable fluorophores (Supplementary Fig. 1). The contrast between photoactivated and background fluorescence, evident in unmasked images, was generally high, thus minimizing the risk that we lost substantive information in the masking process.

Electrophysiology. Electrophysiological recordings were performed on flies 12–48 h after eclosion. Cell bodies were targeted for patch recording by their fluorescence from CD8-GFP or, in some cases, C3PA-PAGFP that was minimally photoactivated to weakly label soma above the background fluorescence. We obtained similar response profiles for neurons expressing either fluorophore.

The PNs that innervate the DA1 glomerulus reside in two clusters of cell bodies that surround the antennal lobe. The cell bodies of Fru+ cholinergic DA1 PNs are characteristically positioned lateral to the antennal lobe, whereas the cell bodies of Fru− DA1 PNs lie ventral to the antennal lobe. A third cluster of PNs frames the dorsal aspect of the antennal lobe but contains no DA1 PNs. We used the stereotyped position of the PN cell bodies relative to the antennal lobe to target these neurons in Gal4 lines that label more than one glomerulus. DA1 PNs are the only lateral PNs labelled in MZ19-Gal4 and fru^{GAL4} lines. We identified VA1d PNs as soma labelled by MZ19-Gal4 that reside in the dorsal PN cluster. Similarly, we identified VA1lm PNs as soma labelled by fru^{GAL4} that reside in the dorsal PN cluster. GH146-Gal4 labels about 60% of PNs that innervate about 35 glomeruli[10–12]. We recorded from random PNs that innervate glomeruli other than DA1 by targeting GH146+ PNs in the dorsal PN cluster.

DC1 neurons were targeted for recording in fru^{GAL4} flies. DC1 somata are readily identified even without photactivation by their characteristic position and fasiculated projections in the lateral horn. We did not record from DC1 neurons in flies in which the DC1 cluster was not well separated from neighbouring lateral horn clusters.

The DN1 cell body is positioned at the midline in the ventral portion of the posterior brain. Unfortunately it was not possible to distinguish this neuron unequivocally from a pair of neighbouring Fru+ neurons by anatomy alone. However, we could differentiate DN1 on the basis of intrinsic membrane properties: intracellular recordings reveal that somatic current injection in DN1 elicits action potentials that have a characteristically lower amplitude (about 10–12 mV) than observed for either of the pair of neighbouring neurons (more than 20–30 mV). Nevertheless, after all recordings of DN1 were completed, we filled the neuron (by electroporation of Texas Red dextran) to confirm its distinct projection pattern in the lateral triangle and SMP tract.

We recorded odour-evoked responses from neurons within the cVA circuit in an intact fly preparation performed essentially as described previously[13]. Flies were immobilized beneath a thin acrylic partition. The angle of the head beneath the partition was adjusted to permit access to DA1 PNs and DC1 neurons on the anterior side of the brain or descending neurons on the posterior side of the brain. Either the anterior or posterior side of the brain was exposed by removal of the overlying cuticle with fine forceps; the fly otherwise remained fully intact. The response of neurons to direct stimulation of glomeruli was recorded in an explant preparation in which the brain was dissected from the head capsule, cleaned of

attached tracheal fibres and pinned with fine tungsten wires onto a thin sheet of Sylgard. In both preparations, the perineural sheath was weakened by treatment with 1–2 mg ml^{-1} collagenase for 1–2 min. The exposed neuropil was then continuously perfused (about 2–3 ml min^{-1}) with external saline (108 mM NaCl, 5 mM KCl, 2 mM $CaCl_2$, 8.2 mM $MgCl_2$, 26 mM $NaHCO_3$, 1 mM NaH_2PO_4, 5 mM trehalose, 5 mM sucrose, 5 mM HEPES, osmolarity adjusted to 275 mosM). The external saline was continuously bubbled with 95%O_2/5% CO_2 and reached a final pH of 7.3.

We performed loose patch recordings on PNs and DC1 neurons by using glass electrodes (7–9 MΩ) filled with external saline and connected to a patch-clamp amplifier (Axon MulticlampB; Axon Instruments) in voltage-clamp mode held at the zero-current potential. Loose patch recordings were obtained by gentle suction to form seals of 40–90 MΩ. Data were band-pass filtered at 100–400 Hz and digitized at 10 kHz. Spikes were detected by the application of a threshold function in Clampfit (Molecular Devices) or by applying a continuous wavelet transform to the raw data in a custom program written in MATLAB (Mathworks). Because of the small size of DC1 cell bodies (diameter 3–4 μm), it was not always possible to maintain loose patch seals for multiple trials of each stimulus. Each measurement is therefore the average of one to three trials per cell.

Intracellular recordings of DN1 were performed with patch electrodes (15–18 MΩ) filled with internal saline (130 mM potassium aspartate, 8 mM KCl, 0.2 mM $MgCl_2$, 5 mM sucrose, 10 mM HEPES pH 7.3, 10 mM EGTA). Recordings were terminated if R_{input} was less than 250 MΩ. In some recordings, we injected hyperpolarizing current (less than 15 pA) to bring the soma to a resting potential of −50 to −55 mV and compensate for leak conductance. Responses of DN1 under these conditions were similar to those observed by loose patch recording. Voltage traces were acquired in current-clamp mode, digitized at 10 kHz and filtered at 5 kHz.

Functional imaging. Optical imaging experiments were performed in flies that contained one copy of fru^{GAL4} driving expression from two or three copies of the UAS-GCaMP3 transgene. Fly brains were dissected and imaged in a modified external saline containing 1–2 mM $MgCl_2$, a condition that we found enhances fluorescence changes reported by GCaMP3 but largely maintains the specificity of glomerular stimulation (data not shown). Images were acquired at 925 nm at 2 Hz. We recorded four trials of fluorescence changes elicited in response to glomerular stimulation for each lateral horn cluster. We averaged these trials and then calculated the normalized changes in fluorescence intensity as $\Delta F/F = 100(F_n - F_0)/F_0$, where F_n is the fluorescence of the nth frame and F_0 is the average baseline fluorescence of the eight frames before stimulation.

Odour stimulation. Odour stimulation was achieved by directing a continuous stream (about 300 ml min^{-1}) of ultrapure-grade air through a 2-mm diameter glass tube directed at the fly's antenna. At a trigger, a solenoid valve controller system (Parker Hannifin Corporation), redirected the air stream from a blank cartridge to one containing various dilutions of cVA or an odorant mix. cVA (Pherobank) or odorants were diluted in paraffin oil (Fluka). The odorant mix consisted of a 1:1,000 dilution of each of ten odorants (benzaldehyde, cyclohexanol, geranyl acetate, 2-heptanone, hexan-1-ol, ethyl 3-hydroxybutarate, 3-methylbutan-1-yl acetate, octan-3-one, methyl salicylate and propionic acid). Each odour cartridge was made by placing 10 μl of the odour stimulus on filter paper and inserting it into a 10-ml glass vial.

Single glomerular stimulation. Glass stimulating electrodes were pulled to a resistance of 7–8 MΩ when filled with 2 mM acetylcholine (Sigma) in external saline. Stimulating electrodes were positioned into the centre of superficial glomeruli viewed under IR-DIC optics. Although we can observe the boundaries of glomeruli under these conditions, we lack the optical depth and clarity necessary to identify stimulated glomeruli unequivocally in this preparation. This problem is compounded by differences in orientation of the antennal lobe from animal to animal. However, glomeruli marked by fru^{GAL4} (DA1, VA1lm and VL2a) or MZ19-Gal4 (DA1 and VA1d) could be identified. We note that the Fru+ VL2a glomerulus is not sufficiently superficial to be effectively impaled with a stimulating electrode in our preparation; it was therefore not tested. Square current pulses (200 or 500 ms long) generated by a Grass stimulator were applied to excite the impaled glomerulus. PNs are probably depolarized through a combination of electrical and chemical excitation, because stimulation with saline alone elicits action potentials, although at lower frequency than in the presence of neurotransmitter.

We examined the specificity of glomerular stimulation by comparing the responses evoked in cognate and non-cognate PNs (Fig. 2b). We first recorded the response of a genetically marked PN to stimulation of its cognate glomerulus over a range of voltages to establish a baseline response. Without moving the stimulating electrode we then recorded from a non-cognate PN innervating a different glomerulus. This non-cognate PN was stimulated at increasing voltages until action potentials were evoked. In rare cases, if no response could be elicited by even strong stimulation (10 V) of the non-cognate glomerulus, the recording was terminated. In this way a lack of response could never be ascribed to inadequate formation of a loose patch seal.

We examined the specificity with which DC1 neurons respond to stimulation of different glomeruli by first recording the response of a DC1 neuron to DA1 stimulation over a range of voltages (Fig. 2e). We then repositioned the stimulating electrode into other superficial glomeruli located throughout the antennal lobe, usually beginning with the neighbouring VA1d and VA1lm glomeruli. Given that fewer than about ten DA1 action potentials are required to bring a DC1 neuron to threshold (Fig. 2g), we expect that even weak stimulation of any single glomerulus should be sufficient to elicit a suprathreshold response in a DC1 neuron. Nevertheless, to account for intrinsic differences in the levels of glomerular excitation evoked by iontophoresis of acetylcholine (Fig. 2b), we stimulated other glomeruli at higher voltages (4 V). At the end of all experiments we recorded the response of the DC1 neuron to stimulation of the DA1 glomerulus again, to ensure that there was no loss in responsivity over time.

Two-photon laser-mediated microlesioning. DC1 processes form a tightly fasciculated bundle as they exit from the lateral horn, allowing us sever most of these processes with a relatively small lesion. We initially observed DC1 neurons expressing either GCAMP3 of CD8-GFP at 925 nm. We defined a lesion target (about 2 μm × 3 μm) in a single z plane at high zoom (×8) centred on the DC1 processes proximal to where they bifurcate and innervate the lateral triangle. We then applied one to four pulses of intense 800-nm light (75–90 mW at the back aperture) until we first observed the formation of a small transient cavitation bubble. Under these conditions, DC1 processes are acutely and completely severed as revealed by their physical discontinuity and the loss of DC1 cell body responses to DA1 stimulation.

We examined the requirement of the DC1 cluster to mediate the response of DN1 elicited by DA1 stimulation, by initially establishing intracellular recordings of DN1. We then recorded the average membrane potential changes evoked by DA1 stimulation (five trials) with the circuit intact to establish a baseline. We then lesioned the DC1 processes. Microlesioning of DC1 neurons affects neither the input resistance nor the action potential threshold of DN1, suggesting that the microlesioning process does not affect the intrinsic excitability of the neuron. After microlesioning we typically waited for 5–10 min (and up to 25 min) to record the average responses (five trials) of DN1 to DA1 stimulation to ensure that we were not confounded by reversible changes in responsivity.

Labelling neurons through electroporation of dye. Dye filling of both glomeruli and single neurons was accomplished through electroporation of highly concentrated (100 mg ml^{-1}) 3,000-Da Texas Red dextran (Invitrogen). Pulled glass electrodes were back-filled with the dextran dye and then connected to the output of a stimulator (Grass). We then positioned the dye-filled electrode in the centre of a single glomerulus or adjacent to a single cell body. Voltage pulses (20–30-V pulses, 5 ms, 1 Hz) were applied until the dye became visible in distal neural processes.

Immunochemistry and characterization of DC1 neurotransmitter. Brains were fixed in 4% paraformaldehyde for 30 min and then incubated for 24 h at 4 °C in one or more of the following: nc82 antibody (Developmental Studies Hybridoma Bank) at 1:10 dilution, anti-GABA antibody (Sigma) at 1:500 dilution, anti-choline acetyltransferase antibody (Developmental Studies Hybridoma Bank) at 1:100 dilution, anti-vesicular glutamate transporter antibody (a gift from A. DiAntonio) at 1:5,000 dilution, anti-tyrosine hydroxylase antibody (Millipore) at 1:500 dilution or anti-serotonin antibody (Sigma) at 1:500 dilution. Brains were then washed and incubated in secondary antibody (Alexa Fluor 546 or Alexa Fluor 633 anti-mouse or anti-rabbit (Invitrogen) at 1:500 dilution) for 2 h at 22 °C. The samples were mounted in Vectashield (Vector Laboratories) before being imaged on a Zeiss 510 confocal microscope.

30. Crameri, A., Whitehorn, E. A., Tate, E. & Stemmer, W. P. Improved green fluorescent protein by molecular evolution using DNA shuffling. *Nature Biotechnol.* **14,** 315–331 (1996).
31. Pedelacq, J. D., Cabantous, S., Tran, T., Terwilliger, T. C. & Waldo, G. S. Engineering and characterization of a superfolder green fluorescent protein. *Nature Biotechnol.* **24,** 79–88 (2006).
32. Stocker, R. F., Heimbeck, G., Gendre, N. & de Belle, J. S. Neuroblast ablation in *Drosophila* P[GAL4] lines reveals origins of olfactory interneurons. *J. Neurobiol.* **32,** 443–456 (1997).
33. Ito, K. *et al.* The organization of extrinsic neurons and their implications in the functional roles of the mushroom bodies in *Drosophila melanogaster* Meigen. *Learn. Mem.* **5,** 52–77 (1998).